Measurements of differential cross sections in π^+p backward elastic scattering between 1.25 and 2.0 GeV/c

R. J. Ott,* J. M. Trischuk, and J. Va'Vra†
Physics Department, McGill University, Montreal, Canada

T. J. Richards‡
Physics Department, Saint Louis University, St. Louis, Missouri 63103

L. S. Schroeder§
Institute for Atomic Research and Department of Physics, Iowa State University, Ames, Iowa 50010
(Received 28 March 1977)

As part of a program of measurements of the πp system we have measured the backward differential cross section for π^+p elastic scattering at 16 momenta from 1.25 to 2.0 GeV/c inclusive. The angular region covered is -0.46 to -0.97 in $\cos\theta_{\text{c.m.}}$. The high resolution in u of 0.03 to 0.04 (GeV/c)^2, together with good statistics, enables a detailed examination of the momentum and angular dependence of structure in this channel. The data are compared with distributions from other experiments and with the most recent phase-shift fit.

INTRODUCTION

As part of a program of measurements of backward elastic scattering cross sections in the πN system,[1,2] we have measured angular distributions in the π^+p elastic channel at 16 momenta from 1.25 to 2.0 Gev/c. The experiment was performed using a secondary pion beam produced by a slow extracted proton beam at the Berkeley Bevatron. The momentum bite of the beam was $\pm 0.5\%$ and the mean momentum was measured to $\pm 0.5\%$.

THE EXPERIMENT

The experimental apparatus is described in previous publications.[1,2] The method used in the investigation was a double-arm telescope of scintillation counters to measure the angle-angle correlation of elastically scattered particles. A magnet was used in the proton (forward) arm of the system to reduce background from inelastic processes. The main difficulty in this investigation, in comparison to the previously reported π^-p experiments, was the problem of separating the incident pion beam from the residual protons left after the primary production target. The separation of protons from beam pions was accomplished by time of flight, and this limited the maximum beam momentum to <2.0 GeV/c. At energies close to 2.0 GeV/c this problem also implied large corrections to the number of beam pions used in normalizing the data. These problems will be discussed later. A further difficulty was the separation of the unscattered beam from the forward proton detectors, and this limited the values of $\cos\theta_{\text{c.m}}$ at which the cross section was measured for momenta near 2.0 GeV/c.

SEPARATION OF ELASTIC EVENTS

The data-analysis procedure is similar to that described in the preceding paper.

Three criteria were used to separate elastic from inelastic events. The first was the pion-proton angle-angle correlation, which showed clear elastic peaks on top of a smooth background.

Secondly, we measured the time of flight (TOF) between the two particles detected. The timing resolution achieved for particles entering the pion and proton counters was typically ± 0.7 nsec. As the phototubes were mounted on the top of the proton counters and on the bottom of the pion counters, a crude coplanarity could be imposed on the trigger. A total TOF window of 9 nsec was used in data collection, divided into six regions of 1.5 nsec each using the binary output of a digitizing system. The elastic peak shows up strongly in the central TOF bins and not in the extremes of the TOF gate. Hence, we could reduce the effective TOF gate in the off-line analysis to 4.5 nsec and so reject much of the inelastic background in the data. We have studied the effects of using data in the extra TOF bins and find no evidence of contribution to the elastic signal from these bins.

The third criterion used was the examination of the shape of the inelastic background to verify that we could subtract this component simply from elastic data without bias. Using extra counters surrounding the hydrogen target outside the apertures of the two detection arms, we were able to accumulate data with more than two charged particles in the final state simultaneously with the elastic data taking. For these data the distributions of the particle detected in the proton arm for any triggered pion counter were always smoothly varying showing that it would be reasonable to subtract a smoothly varying background from the elastic peak.

Target-empty data were also taken at each incident pion momentum. Hence, it was possible to extract elastic events from background for each pion counter and from these events obtain differential cross sections.

CORRECTIONS TO THE CROSS SECTIONS

The differential cross sections for each pion counter were calculated using the formula

$$\frac{d\sigma}{d\Omega_i}=C_i\,\frac{N_i}{N_\pi N_p \Delta\Omega_i},$$

where N_i is the number of elastic events in the ith pion counter, $\Delta\Omega_i$ is the solid angle of the ith pion counter, $N\pi$ is the number of beam pions incident onto the target, N_p is the number of protons in the liquid hydrogen, and C_i is the correction factor. C_i was broken down into the following components: (a) lepton contamination in the beam, (b) nuclear absorption, (c) pion-decay correction, (d) beam randoms, (e) dead-time losses, (f) counter inefficiencies, and (g) losses due to two or more pion counters firing.

(a) A threshold gas Čerenkov counter was used to determine the fraction of leptons in the beam. The counter was placed close to the target so that corrections due to decays after the counter were very small (<1%). The counter was capable of measuring the electron and muon contamination. This was done at several momenta, and interpolation was used to obtain estimates of the contamination at all momenta. The counter was not left in the beam during data taking as it seriously degraded the quality of the beam at the target.

Approximately 80% of the beam consisted of protons. These were eliminated from the trigger by time of flight up to an incident momentum of 2 GeV/c. Using the estimated time-of-flight resolution of ± 0.75 nsec on the timing counters we calculate a proton contamination of <1% at 2 GeV/c. This was confirmed by Čerenkov-counter measurements.

(b) The nuclear absorption of the beam in the last counter of the beam hodoscope, in the air, target walls, and liquid hydrogen was estimated to be ~1% in total. Similar estimates were made for the scattered particles, considering the absorption in air, liquid hydrogen, target walls, and scintillator. The effective cross section used in the calculations was the total cross section for absorption in the various materials. The error due to an overestimate in the absorption cross section was of the order of 2%. The correction for the absorption of scattered particles was 7–12%.

(c) The decay correction was estimated using both hand calculations and Monte Carlo techniques. In the latter, assuming an initial shape for the differential cross section equal to the experimental shape, we have estimated the correction to be $(0.0\pm1.0)\%$.

(d) The beam randoms rate, particularly at the higher pion momenta, introduced a large correction to the absolute cross sections. The beam rates in the time-of-flight counter were typically 1–1.5 MHz, whereas the rest of the telescope counted at approximately 20% of this rate. Hence, there was a large random-coincidence rate arising from protons counting in the time-of-flight counter and either protons or pions counting in the rest of the beam telescope. Detailed calculations of these effects as a function of momentum were done, using the single- and multiple-counter rates measured in the beam telescope. The correction factors varied from 1.2 to 1.9. The errors on these factors were estimated to be ± 5 to $\pm 25\%$.

(e) With the high instantaneous rates in the beam it was necessary to estimate the dead-time losses due to the beam telescope timing resolution. The microscopic duty factor of the beam was estimated to be 20%, determined by two independent measurements. Typically, the counters in the beam telescope had an overall dead time of 20 nsec. Since the only relevant loss was caused by two beam *pions* (not protons) coming within the resolving time of the system, we estimate the dead-time correction to be 3% with an uncertainty of $\pm 3\%$.

(f) The detection efficiency of the counters was >99.8%. However, the gaps between counters in the three main hodoscopes were non-negligible owing to wrapping. We estimate the correction to the data from these effects to be 1.5%.

(g) The hardware trigger rejected all events in which two pion counters were set, causing an accidental loss of elastic events. The corrections due to this effect were independent of beam rate, being $2.5\%\pm1\%$. The overall systematic errors were dominated by the errors on the estimation of the randoms rate in the beam as seen in Table I. The size of these errors contributes to large uncertainties in the overall normalizations, although the relative normalization at each momentum is known to better than $\pm 5\%$.

SOLID ANGLES

We have used a Monte Carlo program to estimate the solid angle corresponding to each angular bin. This program simulated the elastic scat-

TABLE I. The overall systematic errors and the correction factors to the π^+p differential cross sections.

Correction	Factor	Error
Lepton contamination	1.02–1.11	±2%
Absorption of the beam	1.01	±1%
Absorption of scattered particles	1.07–1.12	±2%
Pion decay	1.00	±1%
rf-structure losses	0.95–0.98	±3%
Pion-counter doubles	1.025	±1%
Beam randoms	1.18–1.90	±15%
Counter inefficiencies (including gaps in arrays)	1.015	
Solid-angle uncertainties		±3%
Uncertainty in liquid-hydrogen mass		±3%
Total	1.29–2.43	±15%

tering process and tracked the final-state particles into regions of solid angle representing the detection apparatus. The trigger criterion was imposed on the simulated data. The beam momentum was uniformly randomized within the calculated momentum bite (±0.5%). The target interaction point was estimated assuming a uniform distribution longitudinally and a Gaussian distribution laterally—1.3 cm horizontally by 0.6 cm vertically, full width at half maximum. The beam divergence of ±12 mrad was obtained from a beam-tracking program. Multiple Coulomb scattering of the final-state particles in all materials was included. The particle energy losses were small enough to be considered negligible.

The solid angles were generated at several momenta and then fitted with a low-order polynomial as a function of angle and momentum to obtain values at all the momenta at which data were taken.

Typically the solid angles were 3–12 msr and were estimated to ±2% to ±4%. The Monte Carlo program was also used to predict the positions and widths of the elastic peaks and aided the subtraction of inelastic background from the elastic data.

CROSS-SECTION DATA

Table II lists our differential cross-section data as a function of beam momentum and center-of-mass scattering angle. Figure 1 shows the differential cross section at six momenta spread throughout the momentum range covered by this experiment. The main features of the data are the dip in the cross section in the region $-0.8 < \cos\theta_{c.m.} < -0.9$ and the peak in the cross section near $\cos\theta_{c.m.} = -1.0$.

Figure 2 shows our differential cross sections at six momenta compared with data from the experiments of Abe *et al.*,[3] Carroll *et al.*,[4] and Kalmus *et al.*[5] The agreement between our data and other data is always excellent in terms of the relative shape of the cross-section variation. However, there are large normalization differences which cannot easily be explained. In particular, below 1.667 GeV/c our data normalization agrees well with that of Abe *et al.* Above this momentum their cross sections are a factor of two larger than ours throughout the angular range. At nearly all momenta where both we and Carroll *et al.* have data the agreement is excellent, in particular, at 1.667 GeV/c and 1.768 GeV/c in the region of disagreement with the data of Abe *et al.* The data of Kalmus *et al.* appear to have a different normalization from other sets of data throughout the momentum region covered here. Although we quote a large normalization error on our data of ~±15% this is clearly insufficient to account for the discrepancies seen here.

Figure 3 shows the comparison of our differential cross sections at six momenta with the predictions of the phase-shift analysis of Ayed *et al.*[6] (Saclay 74). We can see that at momenta below 1.6 GeV/c the shape and normalization of the cross sections are predicted accurately by the phase-shift analysis. Above this momentum the phase-shift-analysis predictions are in poor agreement with all data sets discussed here.

Returning to the discussion of the features of the data in this angular range, we note that the main structure, the dip in the cross section in the region $-0.8 < \cos\theta_{c.m.} < -0.9$, first becomes evident at a beam momentum of 1.3 GeV/c. This dip is the well-known constant u' dip at $u' = -0.2$ (GeV/c)^2, where $u' = u - u_{min}$. The dip in the data remains strong up to the highest momentum discussed here (1.917 GeV/c). It is further interesting to note that the cross section on the dip remains roughly constant at 0.75 mb/sr up to 1.4 GeV/c, then drops linearly with beam momentum to reach a value of ~0.08 mb/sr at 1.7 GeV/c. Above this momentum the fall in the cross section slows, reaching a value of ~0.02 mb/sr at 1.917 GeV/c. This dip in the cross section can be explained in Regge terms as a wrong-signature nonsense zero in the N_α nucleon-exchange amplitude.[7] This behavior, consistent with a low-momentum extrapolation of Regge phenomena,[8] is in clear contrast to backward π^-p scattering in the same momentum region. In that case the dom-

TABLE II. Differential cross sections as a function of beam momentum and center-of-mass scattering angle. The errors shown are purely statistical.

P_{beam} (GeV/c)	$\cos\theta_{\text{c.m.}}$	$\frac{d\sigma}{d\Omega}$ $\left(\frac{\mu\text{b}}{\text{sr}}\right)$	P_{beam} (GeV/c)	$\cos\theta_{\text{c.m.}}$	$\frac{d\sigma}{d\Omega}$ $\left(\frac{\mu\text{b}}{\text{sr}}\right)$
1.250	−0.9710	2479 ± 136	1.280	−0.9715	2920 ± 102
	−0.9521	2434 ± 128		−0.9529	2435 ± 89
	−0.9281	2073 ± 113		−0.9293	1949 ± 76
	−0.8998	1254 ± 87		−0.9014	1374 ± 63
	−0.8684	901 ± 73		−0.8705	1059 ± 54
	−0.8428	773 ± 103		−0.8453	818 ± 71
	−0.8240	830 ± 97		−0.8267	793 ± 68
	−0.8026	727 ± 82		−0.8056	787 ± 62
	−0.7785	799 ± 85		−0.7818	736 ± 55
	−0.7514	723 ± 73		−0.7551	769 ± 54
	−0.7213	832 ± 75		−0.7254	786 ± 51
	−0.6882	741 ± 70		−0.6926	732 ± 48
	−0.6519	771 ± 67		−0.6567	831 ± 49
	−0.6120	776 ± 67		−0.6173	954 ± 50
	−0.5695	912 ± 71		−0.5752	958 ± 50
1.316	−0.9721	2487 ± 43	1.371	−0.9729	2843 ± 96
	−0.9538	2090 ± 37		−0.9551	2321 ± 83
	−0.9307	1589 ± 32		−0.9326	1823 ± 71
	−0.9033	1203 ± 27		−0.9060	1320 ± 59
	−0.8729	888 ± 23		−0.8764	1049 ± 50
	−0.8481	748 ± 31		−0.8523	865 ± 66
	−0.8298	697 ± 31		−0.8344	753 ± 61
	−0.8091	681 ± 27		−0.8142	751 ± 58
	−0.7857	568 ± 22		−0.7913	675 ± 51
	−0.7594	617 ± 21		−0.7656	756 ± 50
	−0.7301	686 ± 21		−0.7370	760 ± 49
	−0.6978	665 ± 20		−0.7054	851 ± 48
	−0.6624	731 ± 20		−0.6707	910 ± 48
	−0.6235	755 ± 20		−0.6325	976 ± 48
	−0.5819	821 ± 20		−0.5917	1169 ± 51
				−0.5488	1259 ± 52
1.390	−0.9732	2759 ± 96	1.440	−0.9739	2552 ± 94
	−0.9556	2213 ± 83		−0.9567	2151 ± 82
	−0.9333	1814 ± 71		−0.9350	1611 ± 69
	−0.9069	1370 ± 60		−0.9092	1213 ± 58
	−0.8776	1053 ± 51		−0.8806	1032 ± 51
	−0.8537	823 ± 67		−0.8572	675 ± 61
	−0.8359	829 ± 64		−0.8399	816 ± 65
	−0.8159	762 ± 58		−0.8202	777 ± 59
	−0.7932	762 ± 55		−0.7980	715 ± 53
	−0.7677	793 ± 53		−0.7731	680 ± 49
	−0.7393	848 ± 52		−0.7452	792 ± 50
	−0.7079	867 ± 49		−0.7144	917 ± 50
	−0.6735	960 ± 50		−0.6806	970 ± 51
	−0.6356	1024 ± 50		−0.6433	1075 ± 51
	−0.5950	1059 ± 50		−0.6034	1129 ± 52
	−0.5523	1183 ± 52		−0.5614	1203 ± 52
1.480	−0.9744	2045 ± 85	1.505	−0.9747	1907 ± 66
	−0.9576	1848 ± 76		−0.9581	1421 ± 55
	−0.9362	1301 ± 62		−0.9370	1136 ± 48
	−0.9110	974 ± 51		−0.9120	872 ± 40
	−0.8829	795 ± 46		−0.8842	703 ± 35
	−0.8599	629 ± 58		−0.8615	637 ± 46
	−0.8428	636 ± 57		−0.8447	549 ± 43

TABLE II. (*Continued*)

P_{beam} (GeV/c)	$\cos\theta_{\text{c.m.}}$	$\frac{d\sigma}{d\Omega}$ $\left(\frac{\mu\text{b}}{\text{sr}}\right)$	P_{beam} (GeV/c)	$\cos\theta_{\text{c.m.}}$	$\frac{d\sigma}{d\Omega}$ $\left(\frac{\mu\text{b}}{\text{sr}}\right)$
1.480	−0.8236	526 ± 50	1.505	−0.8259	512 ± 41
	−0.8017	496 ± 45		−0.8039	500 ± 38
	−0.7771	591 ± 46		−0.7796	573 ± 37
	−0.7497	633 ± 45		−0.7524	615 ± 36
	−0.7194	780 ± 47		−0.7224	645 ± 35
	−0.6860	951 ± 50		−0.6893	773 ± 38
	−0.6493	961 ± 48		−0.6529	947 ± 40
	−0.6098	1007 ± 49		−0.6138	987 ± 39
	−0.5683	1090 ± 50		−0.5726	1027 ± 39
	−0.5228	1100 ± 49		−0.5274	1113 ± 40
1.550	−0.9752	1358 ± 58	1.580	−0.9756	1488 ± 55
	−0.9590	1197 ± 50		−0.9596	1184 ± 47
	−0.9384	886 ± 42		−0.9392	853 ± 39
	−0.9139	634 ± 35		−0.9151	668 ± 34
	−0.8866	437 ± 29		−0.8882	532 ± 30
	−0.8643	475 ± 40		−0.8662	442 ± 39
	−0.8478	476 ± 40		−0.8498	444 ± 37
	−0.8291	402 ± 35		−0.8314	386 ± 34
	−0.8078	434 ± 34		−0.8104	420 ± 32
	−0.7839	409 ± 33		−0.7867	430 ± 31
	−0.7572	496 ± 33		−0.7603	450 ± 30
	−0.7277	581 ± 33		−0.7311	636 ± 33
	−0.6951	627 ± 33		−0.6989	691 ± 33
	−0.6592	711 ± 34		−0.6633	756 ± 34
	−0.6207	793 ± 35		−0.6251	920 ± 36
	−0.5800	904 ± 36		−0.5849	955 ± 36
	−0.5354	941 ± 37		−0.5405	943 ± 35
1.667	−0.9766	620 ± 33	1.700	−0.9195	217 ± 17
	−0.9612	521 ± 29		−0.8940	156 ± 14
	−0.9416	382 ± 24		−0.8730	124 ± 18
	−0.9184	358 ± 23		−0.8575	116 ± 16
	−0.8924	215 ± 18		−0.8398	96 ± 16
	−0.8712	192 ± 24		−0.8198	103 ± 15
	−0.8554	176 ± 22		−0.7972	130 ± 14
	−0.8376	186 ± 21		−0.7719	170 ± 15
	−0.8173	177 ± 21		−0.7439	209 ± 15
	−0.7944	205 ± 20		−0.7230	256 ± 16
	−0.7688	220 ± 20		−0.6788	267 ± 15
	−0.7405	292 ± 21		−0.6420	330 ± 17
	−0.7092	338 ± 21		−0.6030	369 ± 17
	−0.6747	385 ± 21		−0.5602	405 ± 18
	−0.6375	490 ± 22		−0.5156	422 ± 18
	−0.5982	513 ± 22			
	−0.5549	524 ± 22			
	−0.5100	570 ± 23			
1.768	−0.9219	106 ± 10	1.816	−0.9234	93 ± 10
	−0.8970	85 ± 9		−0.8990	75 ± 9
	−0.8766	65 ± 11		−0.8790	54 ± 11
	−0.8615	64 ± 11		−0.8642	61 ± 11
	−0.8443	65 ± 10		−0.8473	44 ± 9
	−0.8247	80 ± 10		−0.8281	49 ± 9
	−0.8027	75 ± 9		−0.8064	57 ± 9
	−0.7780	87 ± 10		−0.7821	64 ± 9
	−0.7507	88 ± 9		−0.7552	92 ± 9
	−0.7204	125 ± 10		−0.7254	108 ± 10
	−0.6869	159 ± 10		−0.6924	117 ± 9

TABLE II. (*Continued*)

P_{beam} (GeV/c)	$\cos\theta_{c.m.}$	$\frac{d\sigma}{d\Omega}$ $\left(\frac{\mu b}{sr}\right)$	P_{beam} (GeV/c)	$\cos\theta_{c.m.}$	$\frac{d\sigma}{d\Omega}$ $\left(\frac{\mu b}{sr}\right)$
1.768	−0.6509	185 ± 11	1.816	−0.6569	159 ± 10
	−0.6127	213 ± 11		−0.6192	171 ± 10
	−0.5705	213 ± 11		−0.5776	182 ± 10
	−0.5267	235 ± 11		−0.5343	208 ± 10
				−0.4894	221 ± 11
1.865	−0.9249	57 ± 7	1.917	−0.9265	36 ± 6
	−0.9010	60 ± 7		−0.9031	29 ± 6
	−0.8814	38 ± 9		−0.8838	33 ± 8
	−0.8668	35 ± 9		−0.8695	24 ± 7
	−0.8502	38 ± 8		−0.8532	11 ± 6
	−0.8314	36 ± 7		−0.8347	23 ± 6
	−0.8100	42 ± 7		−0.8138	25 ± 6
	−0.7862	38 ± 7		−0.7903	36 ± 5
	−0.7597	41 ± 6		−0.7643	34 ± 6
	−0.7304	71 ± 7		−0.7354	59 ± 6
	−0.6979	84 ± 7		−0.7034	43 ± 5
	−0.6628	110 ± 7		−0.6689	62 ± 6
	−0.6256	143 ± 8		−0.6322	88 ± 6
	−0.5845	146 ± 8		−0.5917	100 ± 7
	−0.5417	156 ± 8		−0.5494	105 ± 6
	−0.4974	171 ± 8		−0.5056	103 ± 6
				−0.4597	123 ± 7

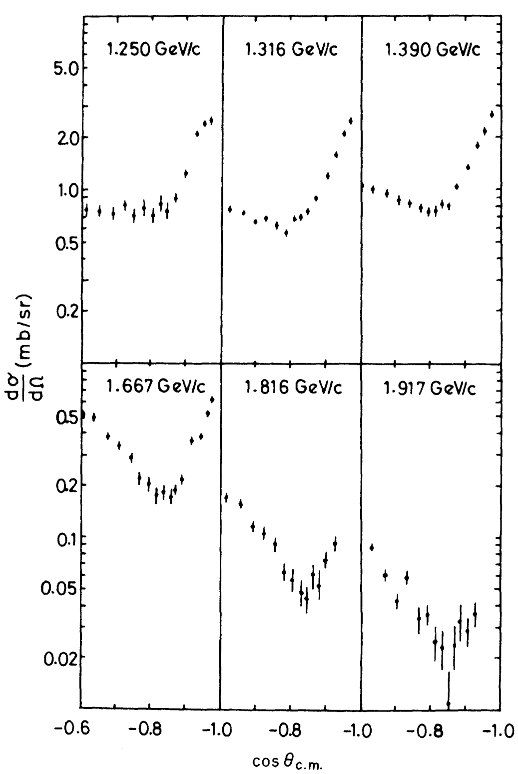

FIG. 1. The differential cross sections in π^+p scattering at 1.25, 1.316, 1.39, 1.667, 1.816, and 1.917 GeV/c.

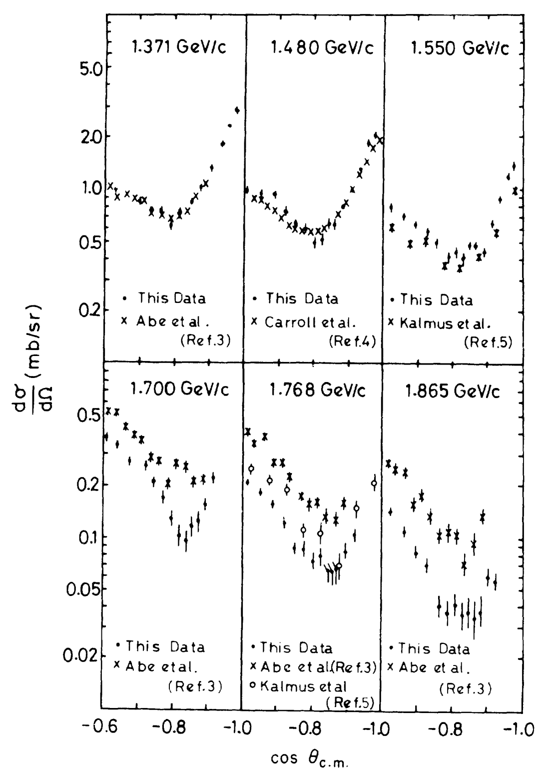

FIG. 2. The comparison of our differential cross sections at 1.371, 1.48, 1.55, 1.7, 1.768, and 1.865 GeV/c with the data of Abe *et al*. (Ref. 3), Carroll *et al*. (Ref. 4), Kalmus *et al*. (Ref. 5).

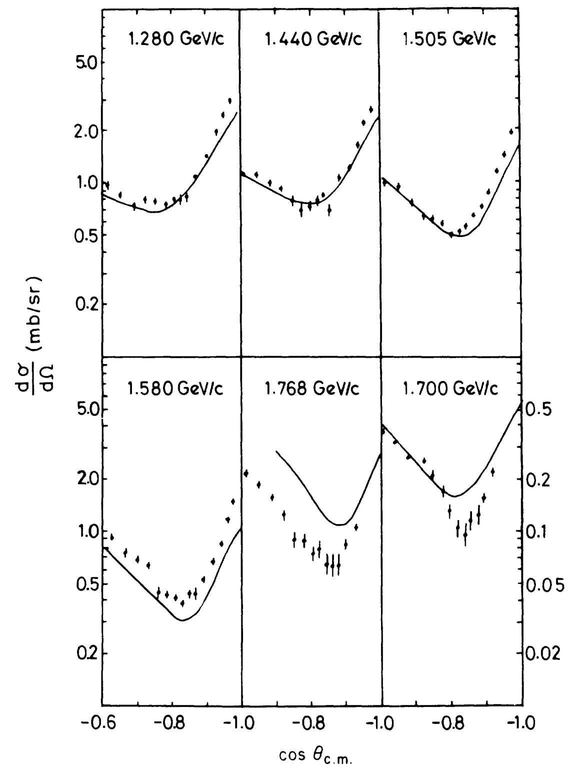

FIG. 3. The comparison of our differential cross sections at 1.28, 1.44, 1.505, 1.58, 1.7, and 1.768 GeV/c with the predictions of the Saclay 74 phase-shift analysis (Ref. 6). (The scale used for 1.7 and 1.768 GeV/c is that on the right-hand side of the figure.)

inance of the individual partial waves is observed to much higher momenta.[2,9]

CONCLUSIONS

We have measured the backward π^+p elastic differential cross section at 16 momenta in the range 1.25 to 2.0 GeV/c. The data show the well-known constant $u' = -0.2$ (GeV/c)^2 dip, which first becomes evident at ~1.3 GeV/c. The cross section in the dip falls linearly with momentum between 1.4 GeV/c and 1.7 GeV/c—the fall is a factor of ten. The comparison of these data with existing data sets shows large inconsistencies in the overall normalization of all data sets; these cannot be explained by the systematic uncertainties quoted. A comparison with the predictions of a recent phase-shift analysis shows good agreement below 1.6 GeV/c. Above this momentum both the predicted shapes and normalizations do not agree well with the data.

ACKNOWLEDGMENTS

We would like to thank the Bevatron staff and in particular Dr. R. Sah for their assistance during the course of this work.

*Present address: Rutherford Laboratory, Chilton, Didcot, Oxon OXII OQX, England.

†Present address: Carleton University, Ottawa, Ontario, Canada.

‡Present address: Research Department, Caterpillar Tractor Company, Peoria, Illinois 61602.

§Present address: Lawrence Berkeley Laboratory, Berkeley, California 94720.

[1]T. J. Richards, D. G. Crabb, R. Keller, J. R. O'Fallon, R. J. Ott, J. Trischuk, J. Va'Vra, and L. S. Schroeder, Phys. Rev. D 10, 45 (1974).

[2]R. J. Ott, J. Trischuk, J. Va'Vra, T. J. Richards, and L. S. Schroeder, Phys. Lett. 42B, 133 (1972).

[3]K. Abe, B. A. Barnett, J. H. Goldman, A. T. Laasaren, P. H. Steinberg, G. J. Marner, D. R. Moffett, and E. F. Parker, Phys. Rev. D 10, 3556 (1974).

[4]A. S. Carroll, J. Fischer, A. Lundby, R. H. Phillips, C. L. Wang, F. Lobkowicz, A. C. Melissinos, Y. Nagashima, and S. Tewksbury, Phys. Rev. Lett. 20, 608 (1968).

[5]G. E. Kalmus, W. Michael, R. W. Birge, S. Y. Fung, and A. Kernan, Phys. Rev. D 4, 676 (1971).

[6]R. Ayed and P. Bareyre, work presented at the Second International Conference on Elementary Particles, Aix-en-Provence, 1973 (unpublished).

[7]V. Barger, F. Halzen, and R. J. N. Phillips, Nucl. Phys. B57, 401 (1973).

[8]E. L. Berger and G. C. Fox, Nucl. Phys. B26, 1 (1970).

[9]F. Halzen, M. G. Olsson, and A. Yokosawa, Nucl. Phys. B113, 269 (1976).